Oxidation of alkenes to 1,2-diols: FT-IR and UV studies of silica-supported sulfonic acid catalysts and their interaction with H2O and H2O2

UNIVERSITÀ DEGLI STUDI DI TORINO

Oxidation of alkenes to 1,2-diols: FT-IR and UV studies of silica-supported sulfonic acid catalysts and their interaction with H_2O and H_2O_2

Raimondo Maggi[a,*], Gianmario Martra[b,*], Calogero Giancarlo Piscopo[a], Giovanni Sartori[a], Gabriele Alberto[b], Salvatore Coluccia[b]

a) "Clean Synthetic Methodology Group", Dipartimento di Chimica Organica e Industriale dell'Università, and Consorzio Interuniversitario 'La Chimica per l'Ambiente' (INCA), UdR PR2, Parco Area delle Scienze 17A, I-43124 Parma, Italy

b) Dipartimento di Chimica IFM & Centro Interdipartimentale di Eccellenza "Nanostructured Interfaces and Surfaces – NIS", Università degli Studi di Torino, Via P. Giuria 7, I-10125 Torino, Italy

Corresponding author:

Prof. Raimondo Maggi

Dipartimento di Chimica Organica e Industriale

Parco Area delle Scienze 17A

I-43124 Parma

Italy

e-mail: raimondo.maggi@unipr.it

phone: +39 0521 905411

fax: + 39 0521 905472

Abstract

Supported sulfonic acids can be employed as efficient catalysts in the dihydroxylation of 1-methylcyclohexene with aqueous hydrogen peroxide, without the use of additional solvents, under mild condition.

The reaction was deeply studied in terms of catalyst, H_2O_2/1-methylcyclohexene molar ratio and percentage of aqueous hydrogen peroxide to achieve the best reaction conditions.

Experimental results, catalytic efficiency and spectroscopy data, allow to advance some hypothesis on the reaction mechanism, based on the interaction, likely via H-bond, of hydrogen peroxide with the sulfate groups resulting from the deprotonation of supported sulfonic acids.

Keywords

Alkene dihydroxylation, hydrogen peroxide, supported catalysts, sulfonic acids, in-situ IR spectroscopy, DR UV-Vis spectroscopy

1. Introduction

Hydrogen peroxide is an ideal oxidant for many reasons: it is cheap, its efficiency is excellent and water is theoretically the sole by-product [1-3]. The activation of aqueous hydrogen peroxide is a challenge that has attracted many research groups in order to perform oxidation reactions, under environmentally friendly conditions [4-5].

From a mechanistic point of view, the activation of hydrogen peroxide can take place in three ways [6]. First, in the presence of metal catalysts, according to the well-known Haber-Weiss reaction, involving the hydroxyl radical, that frequently leads to unselective processes in organic synthesis [7]; second, in the presence of a base, through the formation of the strong HOO^- nucleophile, that can oxidize, for example, electrophilic alkenes [1]; third, according to the heterolytic oxidation process, that is probably the most important reaction from a synthetic point of view [8].

In the presence of catalysts containing different transition metals such as Ti, W, Mn, Re and Sn [9-13], hydrogen peroxide undergoes efficient oxidation reactions, for example alkene epoxidation [14-17], conversion of sulfides into sulfoxides and sulfones [18-21] and Baeyer-Villiger (BV) oxidation of ketones to esters or lactones [22-26]. In all these cases the reaction involves an electrophilic activation of hydrogen peroxide; the same mechanism is reported with fluorinated solvents, as it was clearly shown by Sheldon and Berkessel [27-28].

With regard to the crucial role of peracids added to the reaction mixture or produced in situ from carboxylic acids, many studies are reported in the literature [29]; however the role of different acids such as sulfonic, arsonic and phosphonic acids showing a similar behaviour is not as much studied and needs further deepening. For example,

supported-sulfonic acids were reported to be good heterogeneous and reusable catalysts for the BV oxidation of cyclopentanone [30], and more recently Sato reported a very efficient procedure for the solvent-free dihydroxylation of alkenes with hydrogen peroxide in the presence of Nafion resin [31].

Despite the numerous examples reported in the literature concerning the catalytic dihydroxylation of olefins with hydrogen peroxide [32-34], the selectivity toward 1,2-diols is frequently very low, due to the formation of epoxides, alcohols, ketones, and/or ethers as by-products. Moreover in all the reported synthetic methods the use of chlorohydrocarbons or other organic solvents is required. For these reasons, in continuation of our investigation on the preparation, characterization and use of organic and organometallic catalysts supported onto different materials [34-36,26], we have evaluated the activity of some silica-supported sulfonic acids as heterogeneous catalysts for the dihydroxylation of 1-methylcyclohexene with hydrogen peroxide. In addition, molecular features of the supported acids and of their interaction with H_2O_2 have been investigated by IR spectroscopy in controlled atmosphere and DR UV-Vis spectroscopy of the catalysts in contact with H_2O_2/H_2O solutions.

2. Experimental

2.1 Materials

Toluene, ethanol, acetonitrile, acetone, 1,2-dichloroethane, DMF, 1-methylcyclohexene, bromobenzene, phenyltriethoxysilane, phenylethyltrimethoxysilane, 3-bromopropyltrimethoxysilane (BPTS), chlorosulfonic acid, hydrogen peroxide 30% and 50% and manganese(II) oxide were purchased in the

highest purity available and used without further purification. Methanol was distilled before use.

H_2O (bidistilled), and D_2O (Euriso-top; 99.90%D) were purified *in vacuo* and rendered gas-free by several "freeze-pump-thaw" cycles to be employed in the IR spectroscopic measurements. The same was done for a H_2O_2/H_2O solution (Sigma-Aldrich; ≥ 30%; *Trace* SELECT), that was also used to prepare the slurries for DR UV-Vis spectroscopic investigations.

Gas-chromatographic analyses were accomplished on a TraceGC ThermoFinnigan instrument with a fused silica capillary column SPB-20 from Supelco (30 m x 0.25 mm).

N_2 adsorption-desorption isotherms, obtained at 77 K on a Micromeritics PulseChemiSorb 2705, were used to determine specific surface areas ($S.A._{BET}$), while pore volume and size were calculated by using the BJH model. Before measurements all samples were outgassed at 383 K until a residual pressure 1.0×10-4 Torr (1 Torr: 133.33 Pa).

The surface acidity and surface area of all catalysts were determined by a reported titration method [37] and by the BET method [38] respectively (Table 1).

2.2 Catalyst preparation

The catalysts were synthesized by tethering procedure as reported in the literature [39]. All the catalysts were carefully washed with acetone (3 x 20 mL) and water (3 x 50 mL) and dried for 24 hours at 100 °C before use.

2.2.1 Supported arylsulfonic acids [39]

Silica (8.0 g) was refluxed under stirring for 24 h with phenyltriethoxysilane (2.0 mL, 8.3 mmol) or phenylethyltrimethoxysilane (1.8 mL, 8.3 mmol) in toluene (120 mL), filtered and washed with toluene. The supported phenyl group was then sulfonated by refluxing the functionalized material with chlorosulfonic acid (10 mL, 150 mmol) under stirring for 4 h in 1,2-dichloroethane (60 mL). The solid material was then recovered by filtration and carefully washed with 1,2-dichloroethane (3 x 20 mL), acetone (3 x 20 mL) and water (3 x 50 mL). The catalysts derived from sulfonation of the materials obtained from tethering to silica phenyltriethoxysilane and phenylethyltrimethoxysilane will be hereafter referred to as catalyst A and C, respectively.

A new method was developed for the preparation of the silica supported 4-propoxybenzensulfonic acid (hereafter referred to as catalyst B). A mixture of amorphous silica gel (2.0 g) and BPTS (0.76 mL, 4.0 mmol) in toluene (80 mL) was refluxed, under stirring, for 24 h. The resulting silica supported 3-bromopropane was recovered by filtration and washed with toluene (3 x 50 mL). A mixture of this material (2.00 g) and sodium phenoxide (0.60 g, 6.0 mmol) in DMF (100 mL) was heated to 100 °C under stirring for 24 h. Afterwards the material was filtered off and washed with DMF (3 x 20 mL) and acetone (3 x 20 mL). Finally a mixture of this material (2.0 g) and chlorosulfonic acid (4 mL, 60 mmol) in 1,2-dichloroethane (60 mL) was stirred for 4 h at reflux. The catalyst was recovered by filtration, washed with 1,2-dichloroethane (3 x 20 mL), acetone (3 x 20 mL) and water (3 x 50 mL).

2.3. Catalyst characterization

Infrared spectra of the catalysts were performed in transmission mode on powders pressed in self-supporting pellets ("optical thickness" in the 8-10 $mg \cdot cm^{-2}$ range) and

placed in a quartz IR cell equipped with KBr windows. The IR cell was connected to a conventional vacuum line (residual pressure $p \leq 10^{-5}$ Torr), allowing adsorption/desorption experiments to be carried out in situ. A Bruker Vector 22 spectrometer was employed for spectra collection in the Mid-IR region, and a Jasco 6100 one for selected measurements extended to the Near-IR. In both cases, resolution was 4 cm^{-1}, and a DTGS detector was employed.

All spectra were baseline corrected to remove the contribution of light scattering and were normalized with respect to the intensity of the signals at 1980 and 1870 cm^{-1} due to the combinations of bulk framework modes [40] in order to render differences in intensity independent of differences in the thickness of the pellets.

Mid-IR spectra are reported down to 1250 cm^{-1}, that is the onset of the cut-off due to the fundamental absorptions of the siliceous lattice, that rendered opaque the samples at lower frequency, except for a narrow region (950-850 cm^{-1}, the so-called "silica window"). However, pellets of the catalysts appeared too fragile to be produced so thin to exhibit a reasonable transparency in such range.

Diffuse reflectance (DR) UV-Vis spectroscopy measurements were performed with a Cary 5000 spectrophotometer, equipped with an integrating sphere internally coated with Spectralon®. The same material was used as reference for the collection of the background baseline. The samples, in the form of powder, were put on a quartz optical window, that was the bottom of a cylindrical cell, closed by screwing a piston, pressed toward the powder by a spring. The amount of sample was dosed in order to form a layer ca. 3 mm thick, to extinguish the radiation path within the powder [41]. The samples were investigated both in air and in the form of concentrated slurries, obtained by dropping H_2O or H_2O_2/H_2O solution in proper amounts to obtain an incipient

wetness of the powders. In all cases, the materials were diluted in a 1:30 ratio by weight with highly pure amorphous silica (AOX50, Aerosil), in order to attain the best compromise between the location above the 0% of reflectance of the most intense signals and a satisfactory signal/noise ratio for the weakest ones. The conversion with the Kubelka-Munk function was then attempted, but no longer considered, as the most intense signals exhibited values of the function significantly higher than 1 (for the samples in the form of aqueous slurries), then outside the limits of applicability of such algorithm [41].

2.4. Catalytic tests

The catalytic tests were performed by procedures reported in the notes of table and figures. The general procedure was as follows: a 10-mL round-bottomed flask equipped with a magnetic stirring bar and reflux condenser was charged with the selected solid catalyst (2% mol with respect to 1-methylcyclohexene) and 30% aqueous H_2O_2 (0.86 mL, 8.4 mmol). The mixture was stirred at rt for 10 min, after which 1-methylcyclohexene (0.50 mL, 4.2 mmol) was added. The mixture was heated at 70 °C under stirring for 22 h and then cooled to rt. The catalyst was removed by filtration and washed with methanol (3 x 5 mL); MnO_2 (ca. 100 mg) was added to the solution to destroy any hydrogen peroxide excess. Subsequently, bromobenzene was added as internal standard, the mixture was diluted with methanol and analysed by GC.

3. Results and discussion

3.1. Catalyst characterization

Figure 1 shows the IR spectra of the bare silica and of the three SiO_2-supported catalysts recorded after outgassing at beam temperature (ca. 50 °C) for 1 hour.

PLEASE INSERT FIGURE 1 (now at the end of the manuscript)

Such treatment resulted in the complete desorption of water molecules initially adsorbed from air moisture, as witnessed by the essential invariance of the signal at ca. 1650 cm^{-1} after subsequent exchange with D_2O (inset). Actually, adsorbed water molecules are expected to contribute to that IR band through their deformation (δ) mode, and this contribution should be depleted after exchange with D_2O, and substituted by the δD_2O signal occurring at ca. 1200 cm^{-1} (below the cut-off of the sample).

Focusing on the spectral pattern of the bare SiO_2 support (curve a), on the basis of well assessed literature data [40], the various components can be assigned as follows

• narrow peak at 3740 cm^{-1}: silanols in weak (van der Waals) interaction with neighbours Si-OH;

• shoulder at 3710 cm^{-1}: terminal dangling OH of chains of interacting silanols;

• subband at 3660 cm^{-1}: outer/inner silanols involved in weak hydrogen bonds;

• broad band at 3530 cm^{-1}: silanols involved in stronger hydrogen bonds;

• signals at 1980, 1870 and 1650 cm^{-1}: combinations (the first two) and overtone (the third one) of fundamental silica vibrational modes occurring at lower frequency.

As expected, the last three signals remained unaffected by the tethering of the organic moieties (curves b-d), whereas the peak at 3740 cm^{-1} decreased in intensity, until depletion, as the amount of supported acids increases, and the series of absorptions at lower frequency were overcame by progressively more intense, broad and complex pattern spread over the 3700-2000 cm^{-1} range. It is worthing to note that silanols present

on the surface of the support can be involved in two kinds of events as a consequence of the functionalization with sulfonic acid molecules: i) consumption by reaction with the alcoxysilanes; ii) H-bond interaction with the sulfonic groups, with related frequency downshift and increase in intensity of the ≡SiO-H stretching band.

Of course, the other consequence of the functionalization of the support was the appearance of a series of bands below 1650 cm^{-1}. For the sake of clarity, the assignment of these signals will be reported separately for the alkyl + aryl parts and for the sulfonic group.

Bands due to alkyl + aryl parts. All catalysts (curves b-d) exhibited bands at ca. 1600 and 1410 cm^{-1}, that should be related to 8a and 19b modes (in the Wilson notation [42-44]) respectively, of the aromatic ring (Ar, in the following) [45, 46a, 47]. Their 8b and 19a partner modes, expected to produce significantly weaker absorptions [48, 49], should be then responsible for the components at 1580 cm^{-1} (8b mode) in the spectrum of catalyst C (curve d) and at ca. 1490 cm^{-1} (19a mode) in the spectra of catalysts B and C [45, 46a]. Noticeably, in the case of the catalyst A the 8a band appeared significantly weaker in intensity than expected with respect to the other two catalysts on the basis of the relative amount of supported aromatic species. It can be considered that this band arises from a vibration in which the main dipole moment change is produced by the movements of the substituents on opposite sides of the ring acting in opposition, and then in the presence of one polar substituent or of two substituents with different polarity they should produce quite intense band [48].

Actually, in catalyst A the substituents on the aromatic ring are sulfonic and -$Si(OSi)_3$- groups, exhibiting a significant different polarity. However, the -$Si(OSi)_3$- is in turn directly linked to the support by O-Si bonds. The consequent possible coupling

along the resulting (Ar)-Si-$(OSi)_3$-(support) oscillators could affect the displacement of the Si atom bound to the aromatic ring, with a consequent effect on the dipole moment change. The same argument should hold for the 19a mode, in which the dipole-moment change is produced by the movements of the substituents on opposite sides of the ring, but moving in the same direction.

Furthermore, in the case of catalyst B a weak and broader component is present at 1630 cm^{-1}, that can be due to the overtone of the aromatic 10a γCH mode [45], the fundamental producing the strong band, expected around 815 cm^{-1}, characteristic of *para*-disubstituted benzene rings [46a]. As for the C-H stretching modes, they are responsible for the weak features in the 3100-3000 cm^{-1} range.

The methylene groups of the alkyl links connecting the aromatic rings of catalysts B and C to the support produced the typical series of bands expected for their stretching modes in the 3000-2850 cm^{-1} range, with the ν_{asym} mode splitted in two components (at 2940 and 2900 cm^{-1} in the spectrum of catalyst C, curve d) by Fermi resonance with the overtone of the deformation mode, then expected around 1460 cm^{-1}. Actually, weak bands are present at 1470 and 1475 cm^{-1} for catalyst B (curve c) and C (curve d), respectively. In particular, in the case of catalyst C, the weak component at 1475 cm^{-1} should be due to the -CH_2- group linked to the support, and the other, linked to the aromatic ring, should produce an absorption near 1420 cm^{-1}, likely contributing to the onset of the 19b aromatic mode band.

No specific signals due to Ar-Si, Ar-C, Ar-O bonds were observed, because located below the limit of transparency of the self-supported pellet employed in this study [46a,b].

Bands due to the sulfonic group. The low frequency region of the spectra of the three catalysts is dominated by a broad band in the 1390-1325 cm^{-1} range , assignable to the antisymmetric stretching mode of the O=S=O moiety [50]. Actually, the maximum of this band appeared located at ca. 1370 cm^{-1} for catalyst A (curve b) and at 1355 cm^{-1} for catalyst C (curve d). This is the maximum position also in the case of catalyst B, with a poorly resolved shoulder at ca. 1370 cm^{-1} (curve c). The overall trend suggests that the $\nu(O=S=O)_{asym}$ mode monitors the interaction of the sulfonic group with at least two types of local environment. As for sulfuryl symmetric stretching mode, it should produce a band at ca. 1100 cm^{-1}, well below the limit of transparency of the samples [50].

However, the information on the sulfonic groups is extended by the presence of the spectral features due to the SO-H stretching mode, occurring in the high frequency region. Focussing on the comparison between the bare support (curve a) and catalyst A (curve b), it can be noticed that as a consequence of the surface functionalization, beside the decrease in intensity of the sharp peak at 3740 cm^{-1}, the rest of the νOH pattern is constituted by an asymmetric absorption with maximum similar in position (3510 cm^{-1}) and intensity of that present for the bare silica (3530 cm^{-1}), and a tail extended down to 2800 cm^{-1}. This absorption should results from the superposition of subbands due to O-H stretching of sulfonic groups and silanols. The appearance of the low frequency tail suggests the occurrence of an H-bond interaction between SO-H (expected to act as an H-bond donor) and SiOH (expected to act as an H-bond acceptor). However, the supported acid molecules synthesised starting from phenyltriethoxysilane should be oriented with the sulfuric group pointing away from the support. Thus, the supposed interaction might involve acid molecular moieties formed in pores of the silica support,

where silanols properly located on the facing pore wall could be present. Of course the presence of sulfonic groups involved in weaker H-bond interaction cannot be excluded, and, if present, they should contribute to the part of the asymmetric band close to the maximum at 3510 cm^{-1}. Vice versa, significant amount of sulfonic groups not involved in any interaction should be negligible, as, on the basis of spectra of species entrapped in inert matrices [51] and of theoretical calculations [52], they should absorb at ca. 3560 cm^{-1}.

Focussing on catalyst B, the 3740 cm^{-1} peak appeared slightly less intense, whereas the band at lower frequency, with maximum now located at 3460 cm^{-1}, exhibited a significant increase in intensity, accompanied by the appearance of a shoulder at ca. 3250 cm^{-1} and a partly resolved subband at ca. 2400 cm^{-1}, and a further broadening toward lower frequency, tailing down to ca. 2100 cm^{-1}. Such behaviour monitors the occurrence of stronger H-bond interactions, and the pattern appears typical of the occurrence of a Fermi resonance between overtones of low frequency bending modes, with the continuous distribution of levels resulting from the coupling of ν(A-H···) and ν(AH···B) modes (were A and B represent H-donor and H-acceptor groups, respectively) [53, 54]. In the present case, the role of H-donor is played by the sulfuric groups, whereas the oxygen atoms of surface silanols can act as H-acceptor. Furthermore, it must be considered that in the present case the H-acceptor groups (the silanols) possess an internal mode, the νOH one, that absorbs in the same region, and then can be involved in the coupling. This effect should be responsible for the increase in intensity of the high frequency part of the complex absorption, near the maximum at 3510 cm^{-1}, related to less perturbed oscillators. Indeed, such intensification cannot be ascribed to a higher amount of silanols interacting each other, as, conversely, ≡Si-OH

should have been consumed in a slightly larger amount during the synthesis of the supported sulfonic acid molecules (by assuming the same Si-OH/alcoxide stoichiometry for both phenyltriethoxy- and phenylethyltrimethoxysilane), slightly more numerous in catalyst B than in catalyst A (see Table 1). The stronger interaction between sulfonic groups and silanols should be related to possible orientations of the substituted aromatic ring different from the normal to the surface, because the link to the support through the alkyl moiety, with rotational degree of freedom around the C-C bonds.

Furthermore, the weak feature at ca. 2400 cm^{-1} is similar in position to the low frequency component, with a more intense partner at ca. 2900 cm^{-1}, of the νOH pattern obtained for dehydrated H-NAFION membranes [55], with sulfonic groups interacting each other via H-bonding. Actually, the increase in intensity of this component, and the more clear presence of a broad subband at ca. 3000 cm^{-1}, are the distinctive features of the νOH pattern of catalyst C (curve d), that contains ca. 40% additional supported acid moieties than catalyst B (see Table 1). Other consequences of such increased content in supported molecules are: i) the depletion of the 3740 cm^{-1} peak, indicating that all isolated silanols have been chemically consumed and/or involved in interaction with supported species, and ii) the appearance of sharp minima at 3300 and 3200 cm^{-1}, that might be narrow Evans windows resulting from Fermi resonance between the levels resulting from the coupling of ν(A-H···) and ν(AH···B) modes (see above), and the overtones and combinations of internal modes of the base B involved in the H-bond (in this case, the aromatic sulphate, exhibiting ring modes in the 1650-1550 cm^{-1}), as observed in pyridine/acid zeolites systems [56].

Finally, it can be noticed that the difference in the interaction of sulfonic groups with different neighbours (silanols and/or other sulfonic groups) should affect, other than the

SO-H band, also the S=O ones, and this could partly account for the difference in position and shape of the antisymmetric O=S=O stretching band observed for the three catalysts (see above).

3.2 Interaction of catalysts with H_2O

To probe the acid behaviour of the supported species, the catalysts (and the bare support, for the sake of comparison), where contacted with 20 mbar of H_2O vapour, with the consequent formation of adsorbed multilayers of molecular water [57] and possible proton transfer from sulfonic groups to H_2O molecules (Figure 2).

PLEASE INSERT FIGURE 2 (now at the end of the manuscript)

The admission of water on the bare silica (Figure 2, a,a') simply resulted in the appearance of the bands due to the deformation (δ, at 1630 cm^{-1}) and stretching modes (3730-2800 cm^{-1} range, maximum out of scale), these latter overimposed to the silanols pattern. As expected, the interaction with H_2O molecules heavily affected the peak at 3740 cm^{-1}, as the related groups are now interacting via H-bond with adsorbed species. Nevertheless, a small portion of such signal, with maximum at 3744 cm^{-1} still remained, indicating that some of the surface silanols are so widely distributed to form patches not hydrophilic enough for the adsorption of water [58].

In the case of catalysts (Figure 2, b,b'-d,d'), the additional consequences of the interaction with water were the depletion of the sulfuryl signal in the 1390-1325 cm^{-1} range, and the appearance of a continuous absorption extended from 3500 to 1700 cm^{-1}. This latter is a kind of "fingerprint" of the formation of $H^+(H_2O)_n$ clusters [56], and then probes the transfer of protons to the aqueous layers from $-SO_3H$ groups, converted into $-SO_3^-$, that are expected to absorb below the transparency limit of the samples [56].

Thus, it can be stated that the contact with an aqueous medium results in a complete deprotonation of the sulfonic groups. The same occurred for the materials in contact with air (as some of the UV-vis measurements, see below), with the consequent formation of liquid-like molecular layers by adsorption of air moisture (Figure SI-1 in the SI).

The deprotonation of sulfonic groups is quite relevant for the proposal of the nature of catalytically active species. Indeed, as indicated in the Introduction, supported monoperoxysulfate species, were hypothesized to be active in the selective oxidation of cyclohexene to 1,2-cyclohexanediol [31]. However, the formation of S-O-O-H groups by reaction between sulfuric/sulfonic groups and H_2O_2 requires the presence of a S-O-H moiety, as for instance in the case of sulfuric acid [59, 60, 61]:

$$H_2SO_4 + H_2O \rightarrow HSO_4^- + H_3O^+$$

$$H_2O_2 \rightarrow 2\ OH^\bullet$$

$$HSO_4^- + OH^\bullet \rightarrow SO_4^\bullet + OH^-$$

$$SO_4^\bullet + OH^\bullet \rightarrow SO_4OH$$

Conversely, IR data demonstrated the occurrence of a complete deprotonation of supported sulfonic acids when in contact with an aqueous environment.

3.3 Interaction of catalysts with H_2O_2/H_2O

Similar IR measurements were carried out by admitting the vapour (20 mbar) of a H_2O/H_2O_2 mixture (30% vol H_2O_2) onto the samples.

No specific features related to the interaction of hydrogen peroxide with the species supported on the surface of catalysts were observed (Figure SI-2 in the SI and related

comment) owing to the overwhelming contribution of H_2O, and, likely, the weakness of the H_2O_2-surface species adducts.

Conversely, some information was obtained from the UV-Vis spectra of the systems contacted with H_2O and the H_2O/H_2O_2 solution (Figure 3).

PLEASE INSERT FIGURE 3 (now at the end of the manuscript)

As a first step, the electronic spectra of the materials in the form of an aqueous slurry were collected (Figure 3, panel A). The bare silica exhibited a continuous absorption, progressively increasing in intensity towards the shorter wavelengths, assignable to charge transfer transitions involving metal ion impurities (curve a). Conversely, the spectrum of the much more pure pyrogenic silica employed as diluent, appeared significantly less intense (curve a^0). Overimposed to the feature due to the support, the spectra of the catalysts appeared characterized by a main band at ca. 220 nm (catalysts A and C, curves b,d, respectively) or at ca. 240 nm (catalyst B, curve c), with a weaker partner, exhibiting a partially resolved fine structure, centred at ca. 260 nm (catalyst A and C, curves b,d, respectively) or at ca. 280 nm (catalyst B, curve c). These components can be identified as the primary (*p*) and secondary (α) bands, this latter with the typical vibrational structure, due to transitions involving the π electron system of a benzylic aromatic ring [62]. Their displacement towards longer wavelengths in the case of catalyst B can depend on the presence, as substituent in *para* position with respect the sulfonic group, of an oxygen atom, capable of a larger electron contributing effect than the Si atom and CH_2 present on the aromatic ring in catalysts A and C, respectively. The spectra of the samples in air appeared similar to those of the aqueous slurries in terms of position of the absorption bands, that exhibited a lower intensity (Figure SI-3 in the SI). This was likely due to the increased contribution of light

scattering with respect absorption phenomena in the presence of only some layers of physisorbed water.

Subsequently, the slurries obtained by mixing the samples with the H_2O/H_2O_2 solution were analyzed. All spectra exhibited only a very intense and broad absorption band, with a deep reflectance minimum at ca. 250 nm and a tail towards longer wavelength (Figure 3, panel A'), due to H_2O_2 molecules in aqueous solution [63]. In order to render the spectral profiles independent on difference in intensity due to the not perfect equivalent density of all slurries, and better observe differences in shape, the data have been normalized to the minimum of reflectance.

It can be then noticed that the onset of the absorption of catalysts B and C, appeared shifted towards longer wavelength with respect to both the bare silica support and the catalysts simply in contact with H_2O (Figure 3, panel A' inset). Such feature can be reasonably related to the interaction of H_2O_2 molecules with supported organic species, that, apparently, occurred in a lower extent for catalyst A, the spectrum of which appeared not so different with respect that obtained in the presence only of water. It is of interest to notice that catalyst A exhibited also the lowest catalytic activity, despite the similar content in supported sulfonic acids of catalyst B. Quantum chemical calculations indicate the possibility of the formation of complexes between H_2O_2 and halide anions [64], and then it is proposed that some H-bonding interaction can occur between hydrogen peroxide (acting as an H-donor) and the sulfate groups (acting as H-acceptor) resulting from the deprotonation of supported sulfonic acids. As for the competition with water molecules for the interaction with sulfate groups, it can be recalled that H_2O_2 in aqueous solution is a stronger H-bond donor (but a weaker acceptor) than H_2O [65]. The result of the competition with hydrated H_3O^+ ions should

be the subject of a future modelling, as well as the effect of the sulfate-H_2O_2 interaction on the electronic states of hydrogen peroxide molecules.

The occurrence of such interaction can be relevant for the catalytic process, as the results obtained by Neumann [8] on the selectivity attained in oxidation reactions by using H_2O_2 in perfluorinated alcohol solvents suggested the possibility for an electrophylic activation of hydrogen peroxide via H-bonding. Tentative drawings are reported in Figure 4, where no indication of the H_2O_2 dihedral angle has been reported, intentionally. In general, it is known that hydrogen peroxide has a quite flexible molecular structure, easily distorted by molecular interactions [66, 67], as a result of the only weakly hindered rotation of the OH groups around the O-O bond [66, 68].

PLEASE INSERT FIGURE 4 (now at the end of the manuscript)

3.4. Reaction condition optimization

The activity of the supported sulfonic acid catalysts has been evaluated in the 1,2-dihydroxylation of 1-methylcyclohexene (**1**) with hydrogen peroxide (Table 1) [69].

PLEASE INSERT TABLE 1

The experiments were carried out by adding 1-methylcyclohexene to a suspension of the catalyst in 30% aqueous hydrogen peroxide and by stirring the reaction mixture for 22 hours at 70 °C [70]. The model reaction was first tested with phenylsulfonic acid supported onto amorphous silica, and with the commercially available Amberlyst-15. In all cases 1-methyl-1,2-cyclohexanediol (**3**) was obtained as the major product. The silica supported phenylsulfonic acid (catalyst A, 2% molar ratio with respect to reagent **1**) showed the best activity, affording product **3** in 80% yield and 94% selectivity (Table

1, entry 2). Lower efficiency was observed with Amberlyst-15 (59% yield, 93% selectivity) (Table 1, entry 5).

The catalytic activity of two additional sulfonic acids supported onto silica through arms with different length, namely 4-ethylphenylsulfonic acid and 4-propoxyphenylsulfonic acid, has been successively studied in the reaction performed under the best conditions (2 mol% catalyst, 70 °C, 22 hours, H_2O_2/**1** molar ratio = 2). The best result in terms of yield (90%) and selectivity (96%) of 1-methyl-1,2-cyclohexanediol was obtained with the silica supported 4-ethylphenylsulfonic acid (Table 1, entry 4). The lower activity (80% yield, 94% selectivity) observed for the silica-supported phenylsulfonic acid (Table 1, entry 2) could be ascribed to the fact that the direct anchoring of phenylsulfonic group to the silica surface can partly hamper the availability of the active acid sites with respect the more accessible ethylphenylsulfonic group. The modest activity of the silica supported 4-propoxyphenylsulfonic acid bearing the longest arm (Table 1, entry 3), was tentatively ascribed to the lower stability of the ethereal chain in the reaction medium, that is responsible for some catalyst leaching. Indeed, the elemental analyses of all the utilized catalysts showed that only catalyst B underwent a 45% loss of the total carbon after the first cycle.

The surface area of these catalytic materials seems to be irrelevant in the present reaction; similarly it is impossible to gather a linear correlation between surface acidity and catalytic activity from experimental results reported in Table 1 (see, for example, the poor activity showed by Amberlyst-15 that in water undergoes 60-70% swelling).

In order to evaluate the possible catalytic activity of the bare support, the reaction was performed in the presence of amorphous silica: the siliceous support played no

catalytic role. Similarly hydrogen peroxide itself is not able to oxidize 1-methylcyclohexene.

The influence of catalyst A amount was then evaluated; the results are illustrated in Figure 5.

PLEASE INSERT FIGURE 5 (now at the end of the manuscript)

The system was inert until the catalyst A/substrate **1** molar ratio raised 0.002, then a sharp increase of product **3** yield was observed: 1-methyl-1,2-cyclohexanediol was obtained in 55% yield with a good level of selectivity (93%) by increasing the catalyst A/substrate **1** molar ratio to ca. 0.05. A further yield increase was observed by using a 0.02 catalyst/substrate molar ratio value (80%), whereas with larger amount of catalyst (0.04 catalyst/substrate molar ratio), a lowering in yield due to a non-controllable acid-catalyzed side reactions of the hydroxyl groups was observed (69%).

Concerning the optimum H_2O_2 amount, the best result was achieved with a H_2O_2 /**1** molar ratio = 2; with lower or higher amounts of H_2O_2 product **3** was obtained in lower yield due to the competition of unproductive H_2O_2 decomposition in the first case, and over oxidation reactions in the second one.

The effect of the concentration of the aqueous hydrogen peroxide on the efficiency of the process has been successively evaluated. In a series of experiments, the reaction was carried out in the presence of 1.2, 15, 30 and 50% hydrogen peroxide, by using the same amount of the oxidizing agent. The optimum hydrogen peroxide concentration was found to be 30% (80% yield, 94% selectivity), as the use of 50% H_2O_2 afforded the diol in lower yield (72%) and selectivity (88%), probably due to overoxidation processes; on the contrary, when more diluted solutions of the oxidizing agent were employed, lower

yields and selectivities were detected for the competitive alkene water addition (15% H_2O_2: 49% yield, 80% selectivity; 1.2% H_2O_2: 8% yield, 65% selectivity).

Concerning the efficiency of the hydrogen peroxide under the best reaction conditions (catalyst/substrate molar ratio = 0.02, 30% aq H_2O_2 /substrate molar ratio = 2, 70 °C, 22 h), a value of 65%, calculated as product (mol) per consumed H_2O_2 (mol) × 100, was found.

Addition of a solvent (2 mL) such as toluene, acetonitrile, methanol or water, resulted in a dramatic lowering (<10% yield) or complete inhibition of compound **3** production, irrespective of the polarity. Among the by-products isolated in these reactions, 1-methylcyclohexan-1-ol, due to acid catalyzed addition of water to alkene, and 2-methylcyclohexanone, derived from the isomerisation of epoxide intermediate or from the pinacol rearrangement of 1-methyl-1,2-cyclohexanediol, were recognized in the final mixtures. When methanol was utilized, the expected 2-methoxy-1-methylcyclohexan-1-ol, derived from the reaction of the methanol with the intermediate epoxide, was also isolated in modest yield.

To achieve further information on the behaviour of these catalysts, the reactions with silica-supported phenylsulfonic, ethylphenylsulfonic and propoxyphenylsulfonic acids were analyzed during the first 10 hours under the same reaction condition. Results are reported in Figure 6.

PLEASE INSERT FIGURE 6 (now at the end of the manuscript)

The three catalysts show completely different reaction profiles. Propoxyphenylsulfonic acid (▲) shows a slightly higher initial rate with respect to the ethylphenylsulfonic (■) and phenylsulfonic acids (♦), without any induction period. Instead, variable induction periods were observed with ethylphenylsulfonic and phenylsulfonic acids. IR analyses

indicated that these induction times are not attributable to the production of supported peroxysulfonic acid intermediates.

The catalyst efficiency is expected to be strongly affected by the accessibility of the supported sulfonic acid groups that, in turn, mainly depends on the length of the carbon atom arm that binds them to the support surface, according to the order propoxyphenyl>ethylphenyl>phenyl. However, some further parameters such as the stability and the swelling of the solid catalyst as well as the nature of the solvent affect the efficiency of these catalytic systems.

The higher initial rate is observed with catalyst C (arm: propoxyphenyl). Nevertheless the system reaches a plateau at the modest 55% yield after about 10 hours. As previously showed, we have ascribed this drawback to the low stability of the catalyst in the reaction medium. It is indeed expected that in the present acidic medium the phenyl-alkyl ether linkage could undergo breaking with production of *para*-hydroxybenzene sulfonic acid in solution. The production of an homogeneous arylsulfonic acid accounts for the lack of any induction period and for the modest product **3** final yield. Indeed, our blank experiments confirm that, under homogeneous conditions, *para*-toluensulfonic acid catalyses the reaction with complete conversion of reagent **1** and modest yield (~60%) of product **3** (see Supporting Information).

The induction periods showed with catalyst B (arm: ethylphenyl) and particularly with catalyst A (arm: phenyl) are observed with the as prepared as well the recycled catalysts. We tentatively ascribed this behaviour to the nature of the reaction medium and to its change with the going on of the reaction. Indeed, the reaction mixture is initially triphasic, being constituted of water (H_2O_2), 1-methylcyclohexene and the solid

catalyst. The activation of reagents according to the mechanism reported in Scheme 1 is thus unlikely.

PLEASE INSERT SCHEME 1 (now at the end of the manuscript)

This negative effect is stronger with catalyst A where the phenylsulfonic acid is directly anchored to the silica surface and consequently less available. However, the initial production, even trace amount, of 1-methyl-1,2-cyclohexanediol (**3**) converts the liquid biphasic system into an emulsion followed by the production of a single liquid phase where the reaction is more and more easy.

Consistent with this, the reaction performed with catalyst A in the presence of product **3** (5% mol with respect to reagent **1**) afforded the same product in 45% yield after 8 hours without any induction period (see Supporting Information).

Based on the results reported above, particularly spectroscopic studies, we propose the catalytic mechanism depicted in Scheme 1. In the present aqueous reaction medium the supported benzenesulfonic acid results completely deprotonated affording the supported sulfonate anion in combination with H_3O^+ cation. UV and IR studies gave some information indicating the possible occurrence of a selective H-bond interaction of H_2O_2 (as H-donor) and the sulfonate group (as H-acceptor) in the presence of water, affording the three possible adducts depicted in Figure 4. One of these adducts can transfer one oxygen atom to the alkene moiety affording the corresponding epoxide that in aqueous medium and in the presence of H_3O^+ ion undergoes very fast epoxide ring opening affording the final diol.

The second step, namely the H_3O^+ catalysed addition of a water molecule to the epoxide, seems to be very fast; indeed in a blank experiment we confirmed that cyclohexene oxide was quantitatively converted into the *trans*-1,2-cyclohexanediol in 5

minutes by reaction with water at room temperature in the presence of silica supported 4-ethylphenylsulfonic acid.

At the end the recyclability of the silica supported 4-ethylphenylsulfonic acid catalyst was evaluated in the dihydroxylation of 1-methylcyclohexene. After the reaction, the catalyst was filtered off, washed with water, dried carefully and reused. The yield (and selectivities) were as follows: 1st run: 89 (95), 2nd run: 66 (94), 3rd run: 64 (96), 4th run: 64 (95). A loss of activity was observed during the first run, while maintaining a very high selectivity, whereas from the second cycle the catalyst shows a constant activity.

4. Conclusion

Supported sulfonic acids can be used as eco-efficient catalysts for the dihydroxilation of 1-methylcycloehexene with aq H_2O_2 under mild condition without using any additional solvent. The silica supported 4-ethylphenyl sulfonic acid shows the best activity giving 1-methyl-1,2-cyclohexanediol in 90 % yield and 96 % selectivity. The reaction requires an induction time before the product starts to be present in the reaction mixture. This period can be decreased by suspending the catalyst in aq hydrogen peroxide for two hours before adding the 1-methylcyclohexene. These results, together with the spectral analyses, suggest that the interaction between the catalyst and the hydrogen peroxide give raise to an activation of H_2O_2 molecules, that produce the epoxide intermediate; this epoxide is immediately converted to the diol, by the addition of a water molecule.

Acknowledgments

The authors acknowledge the support of the Ministero dell'Università e della Ricerca (MIUR), Italy, and the University of Parma (National Project "Attivazione ossidativa catalitica e fotocatalitica per la sintesi organica"). The Centro Interdipartimentale Misure (CIM) is acknowledged for the use of NMR instruments. G.A. is recipient of an ASP post-doc fellowship.

References

[1] C. W. Jones, Applications of Hydrogen Peroxide and Derivatives, RSC, Cambridge, 1999.

[2] W. R. Sanderson, Pure Appl. Chem. 72 (2000) 1289-1304.

[3] J. M. Campos Martin, G. Blanco Brieva, J. L. G. Fierro, Angew. Chem. Int. Ed. 45 (2006) 6962-6984.

[4] J.-E. Bäckvall, Modern Oxidation Methods, Wiley-VCH, Weinheim, 2004.

[5] N. Mizuno, Modern Heterogeneous Oxidation Catalysis, Wiley-VCH, Weinheim, 2009.

[6] G. Strukul, Catalytic oxidations with hydrogen peroxide, Kluwer Academic Publishers, Dordrecht, 1992.

[7] N. Uri, Chem. Rev. 50 (1952) 375-454.

[8] K. Neimann, R. Neumann, Org. Lett. 2 (2000) 2861-2863.

[9] M. G. Clerici, G. Bellussi, U. Romano, J. Catal. 129 (1991) 159-167.

[10] C. Venturello, E. Alneri, M. Ricci, J. Org. Chem. 48 (1983) 3831-3833.

[11] D. E. De Vos, B. F. Sels, M. Reynaers, Y. V. S. Rao, P. A. Jacobs, Tetrahedron Lett. 39 (1998) 3221-3224.

[12] W. A. Herrmann, W. R. Fischer, M. U. Rauch, W. Scherer, J. Mol. Catal. 86 (1994) 243-266.

[13] A. Corma, L. T. Nemeth, M. Renz, S. Valencia, Nature 412 (2001) 423-425.

[14] S. T. Oyama, F. W. Bull (Eds.), Mechanisms in Homogeneous and Heterogeneous Epoxidation Catalysis, Elsevier, Amsterdam, 2008.

[15] B. S. Lane, K. Burgess, Chem. Rev. 103 (2003) 2457-2474.

[16] R. Noyori, M. Aoki, K. Sato, Chem. Commun. (2003) 1977-1986.

[17] D. E. De Vos, B. F. Sels, P. A. Jacobs, Adv. Synth. Catal. 345 (2003) 457-473.

[18] R. A. Sheldon, J. K. Kochi, Metal Catalyzed Oxidations of Organic Compounds, Academic Press, London, 1981.

[19] M. Mba, L. J. Prins, G. Licini, Org. Lett. 9 (2007) 21-24.

[20] K. Jeyakumar, D. K. Chand, Tetrahedron Lett. 47 (2006) 4573-4576.

[21] F. Gregori, I. Nobili, F. Bigi, R. Maggi, G. Predieri, G. Sartori, J. Mol. Cat. A: Chem. 286 (2008) 124-127.

[22] G. R. Krow, in L. A. Paquette (Ed.), Organic Reactions, Wiley & Sons, New York, 1993.

[23] M. Renz, B. Meunier, Eur. J. Org. Chem. (1999) 737-750.

[24] G. J. Brink, I. W. C. E. Arends, R. A. Sheldon, Chem. Rev. 104 (2004) 4105-4124.

[25] C. Jimenez Sanchidrian, J. R. Ruiz, Tetrahedron 64 (2008) 2011-2026.

[26] C. G. Piscopo, S. Loebbecke, R. Maggi, G. Sartori, Adv. Synth. Catal. 352 (2010) 1625-1629.

[27] M. C. A. van Viliet, I. W. C. E. Arends, R. A. Sheldon, Chem. Commun. (1999) 821-822.

[28] A. Berkessel, M. R. M. Andreae, H. Schmickler, J. Lex, Angew. Chem. Int. Ed. 41 (2002) 4481-4484.

[29] S. Vayssié, H. Elias, Liebigs Ann. (1997) 2567-2572.

[30] J. Fischer, W. F. Hölderich, Appl. Catal. A: Gen. 180 (1999) 435-443.

[31] Y. Usui, K. Sato, M. Tanaka, Angew. Chem. Int. Ed. 42 (2003) 5623-5625.

[32] M. Sasidharan, P. Wu, T. Tatsumi, J. Catal. 209 (2002) 260-265.

[33] K. Lee, Y. Kim, S. B. Han, H. Kang, S. Park, W. S. Seo, J. T. Park, B. Kim, S. Chang, J. Am. Chem. Soc. 125 (2003) 6844-6845.

[34] A. Hartung, M. A. Keane, A. Kraft, J. Org. Chem. 72 (2007) 10235-10238.

[35] G. Sartori, A. Armstrong, R. Maggi, A. Mazzacani, R. Sartorio, F. Bigi, B. Dominguez-Fernandez, J. Org. Chem. 68 (2003) 3232-3237.

[36] F. Derikvand, F. Bigi, R. Maggi, C. G. Piscopo, G. Sartori, J. Catal. 271 (2010) 99-103.

[37] S. Leveneur, D. Y. Murzin, T. Salmi, J. Mol. Catal. A: Chem. 303 (2009) 148-155.

[38] S. Brunnauer, P. G. Emmeth, E. Teller, J. Am. Chem. Soc. 60 (1938) 309-319.

[39] R. D. Badley, W. T. Ford, J. Org. Chem. 54 (1989) 5437-5443.

[40] A. P. Legrand, A. Burneau, C. Doremieux, A. Foissy, J. Persello J. Gallas, Y. Grillet , P.L. Llewellyn, H. Hommel, J. D'Espinose de la Caillerie, E. Papirer, A. Vidal, H. Balard, F. Ehrburger-Dolle, B. Fubini, The Surface Properties of Silicas, (A. P. Legrand Ed) John Wiley & Sons, Ltd (Uk), 1998.

[41] G. Kortüm, Reflectance Spectroscopy, Springer-Verlag, New York, 1969, p. 239.

[42] E. B. Wilson, Phys. Rev. 45 (1934) 706-714.

[43] E. B. Wilson, Phys. Rev. 46 (1934) 146-147.

[44] E. B. Wilson, J. C. Decius, P.C. Cross, Molecular Vibrations, Dover Pubblications, New York, 1980.

[45] J. H. S. Green, Spectrochim Acta A, 26 (1970), 1503-1513.

[46] N.B. Colthup, L. H. Daly, S.E. Wiberley, Introduction to Infrared an Raman Spectroscopy, Academic Press, New York, 1975, Ch.8, a) pp. 262-267, b) pp.312-340.

[47] H. Takeuchi, N. Watanabe, I. Harada, Spetrochim. Acta A, 44 (1988), 749-761.

[48] L.J: Bellamy, The Infrared Spectra of Complex Molecules, Chapman and Hall, London, 1975, Third Edition p.78.

[49] F. Bonino, A. Damin, S. Bordiga, C. Lamberti, A. Zecchina, Langmuir, 19 (2003), 2155-2161.

[50] D. Detoni, D. Hadzi, Spectrochim. Acta, 11 (1957), 601-608.

[51] A. Givan, L.A: Larsen, A. Loewenschuss, C. J. Nielsen, J. Mol. Struct. 509 (1999) 35-37.

[52] V.M. Zelenkovskii, V. Bezazychnaya, V.S. Soldatov, J. Appl. Spectrosc. 77 (2010) 189-193.

[53] G.C. Pimetel, A.L. McClellan, The Hydrogen Bond, Freeman and Co., San Francisco, 1969

[54] P.D. Schuster, G. Zundel, G. Sandorfy, The Hydrogen Bond- Recent Developments in Theory and Experiment, North Holland Publ. Co., Amsterdam, 1976.

[55] R. Buzzoni, S. Bordiga, G. Ricchiardi, G. Spoto, A. Zecchina, J. Phys. Chem. 99 (1995) 11937-11951

[56] R. Buzzoni, S. Bordiga, G. Ricchiardi, C. Lamberti, A. Zecchina, G. Bellusi, Langmuir 12 (1996) 930-940 and references therein.

[57] M. Takeuchi, L. Bertinetti, G. Martra, S. Coluccia, M. Anpo, Appl. Catal. A: General 307 (2006) 13-20.

[58] V. Bolis, B. Fubini, L. Marchese, G. Martra, D. Costa, J. Chem. Soc. Faraday Trans. 87 (1991) 497-505.

[59] H. Caro, Z. Angew. Chem. 11 (1898) 845-846.

[60] H. Palme, Z. Anorg. Chem. 112 (1920) 97-130.

[61] K. Serrano, P.A. Michaud, C. Comninellis, A. Savall, Electrochim. Acta, 48 (2002) 431-436.

[62] C.N.R. Rao, Ultra-Violet and Visible Spectroscopy, Third ed., Butter Worths, London,1975, p. 61.

[63] R.C. Taylor, P.C. Cross, J. Am. Chem. Soc., 71 (1949) 2266-2268.

[64] M.C. Daza, J.A. Dobado, J. Molina Molina, P. Salvador, M. Duran, J.L. Villaveces, J. Chem. Phys. 110 (1999) 11806-11813.

[65] M.T.C. Martins-Costa, M.F. Ruiz-Lopez, Chem. Phys. 332 (2007) 341-347.

[66] P.A. Giguère, J. Chem. Educ., 60 (1983) 399-401.

[67] T. Minato, D.P. Chong, Can. J. Chem., 61 (1983) 550-552.

[68] M.S. Gordon, J. Am. Chem. Soc., 91 (1969) 3122-3130

[69] The same reaction carried out with SiO_2-SO_3H catalyst (prepared by treating silica with chlorosulfonic acid) afforded an intractable mixture of products.

[70] The addition of H_2O_2 dropwise to a suspension of 1-methylcyclohexene and the catalyst, through a syringe-pump during a period of 15 hours (the reaction mixture was stirred for further 7 hours to allow a total reaction time of 22 h) gave comparable values of yield and selectivity of the desired product with respect to the one-pot addition of hydrogen peroxide.

Figure and scheme legends

Figure 1. IR spectra of samples outgassed at beam temperature (ca. 50 °C) for 1 h: a) bare silica; b) catalyst A; c) catalyst B; d) catalyst C.

Figure 2. IR spectra of samples outgassed beam temperature (ca. 50 °C) for 1 h (curves x, the same as in Figure 1) and in presence of 20 mbar of H_2O vapour (curves x'): a,a') bare silica; b,b') catalyst A; c,c') catalyst B; d,d') catalyst C. The maximum of the main absorption in the high frequency region was out of scale.

Figure 3. DR UV-Vis spectra of slurries obtained by wetting the samples with different aqueous media. Panel A, samples in contact with H_2O: a) bare silica used as support; a^o) highly pure silica used as diluent; b) catalyst A; c) catalyst B; d) catalyst C. Panel A': samples in contact with H_2O_2/H_2O solution: a) bare silica; b) catalyst A; c) catalyst B; d) catalyst C. Inset, zoomed view of the 350-500 nm region, where the spectra (b'),(c'), (d') of the catalysts A,B, and C, respectively, in contact with the H_2O_2/H_2O (the same as in panel A) are compared with the spectrum of the bare silica support in contact with the same medium (curves a', the same as in panel A') and with the spectra (b), (c) and (d) of catalyst the catalysts A,B, and C, respectively, in contact with H_2O (the same as in panel A).

Figure 4. Possible interactions H_2O_2-catalyst

Figure 5. Influence of the catalyst amount on the yield and selectivity in the reaction carried out with SiO_2-(C_6H_4)-SO_3H catalyst.

Figure 6. Yield versus time trend for the reactions carried out with SiO_2-(C_6H_4)-SO_3H (♦), SiO_2-$(CH_2)_2$-(C_6H_4)-SO_3H (▲) and SiO_2-$(CH_2)_3$-O-(C_6H_4)-SO_3H (■) catalysts.

Scheme 1. Possible reaction mechanism.

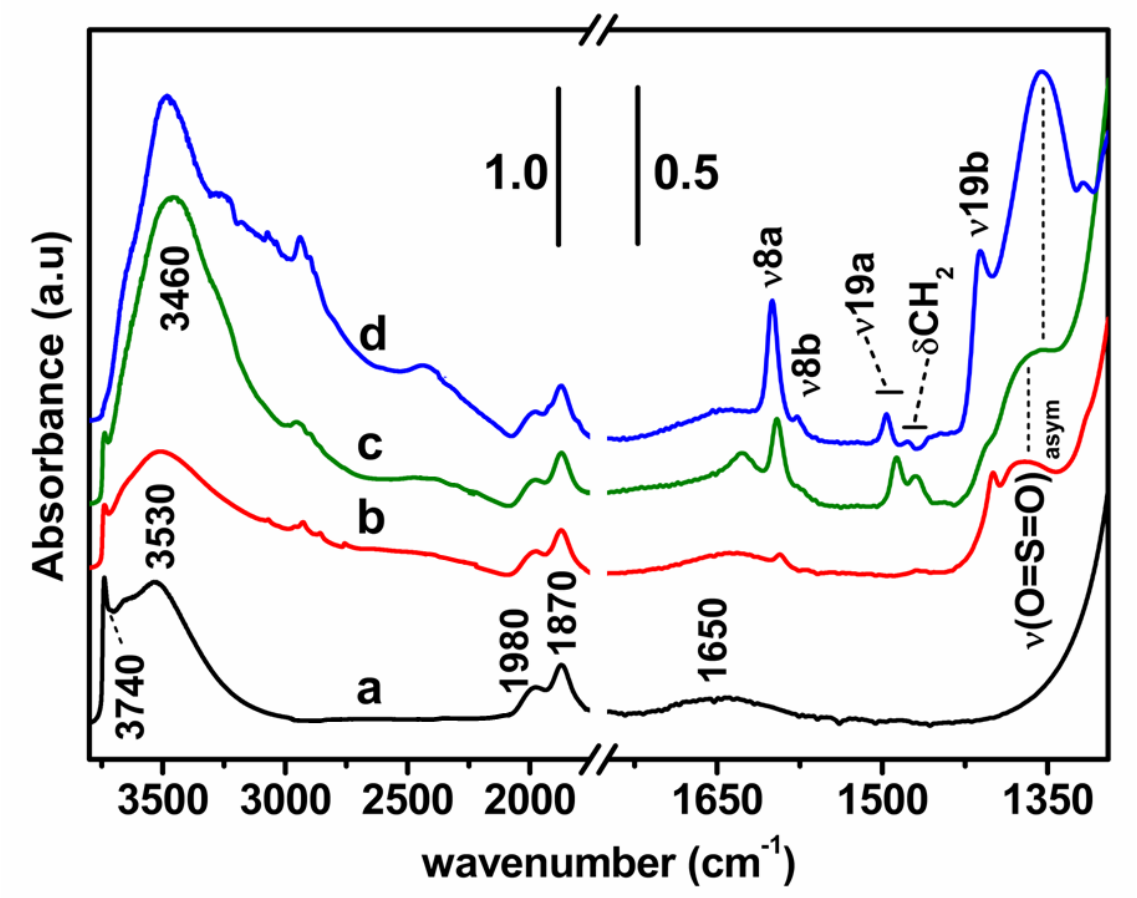
Absorbance (a.u)
1.0
0.5
3460
3530
3740
1980
1870
1650
d
c
b
a
ν8a
ν8b
ν19a
δCH2
ν19b
ν(O=S=O)asym
3500
3000
2500
2000
1650
1500
1350
wavenumber (cm-1)

Figure 1.

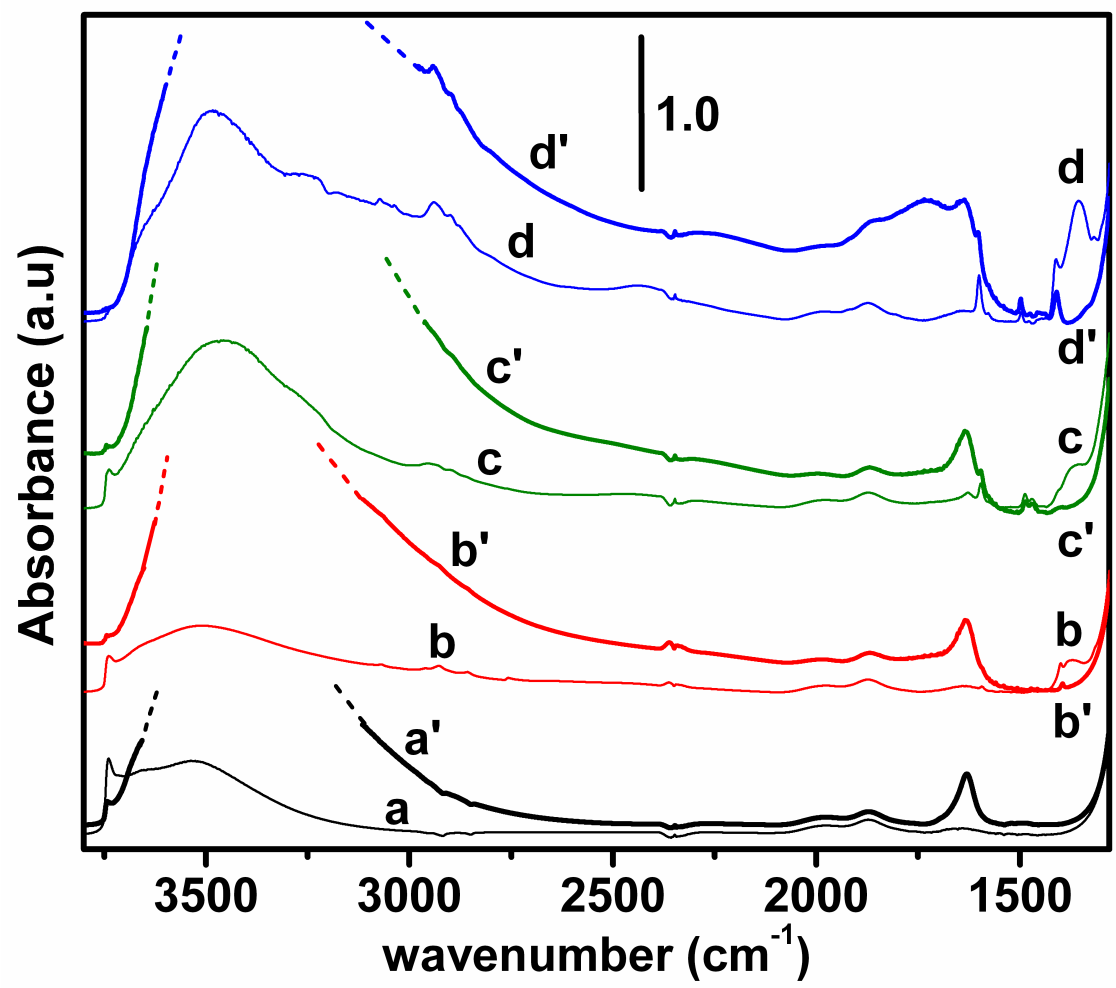
Absorbance (a.u)
1.0
d'
d
d
d'
c'
c
c
c'
b'
b
b
b'
a'
a
3500
3000
2500
2000
1500
wavenumber (cm-1)

Figure 2.

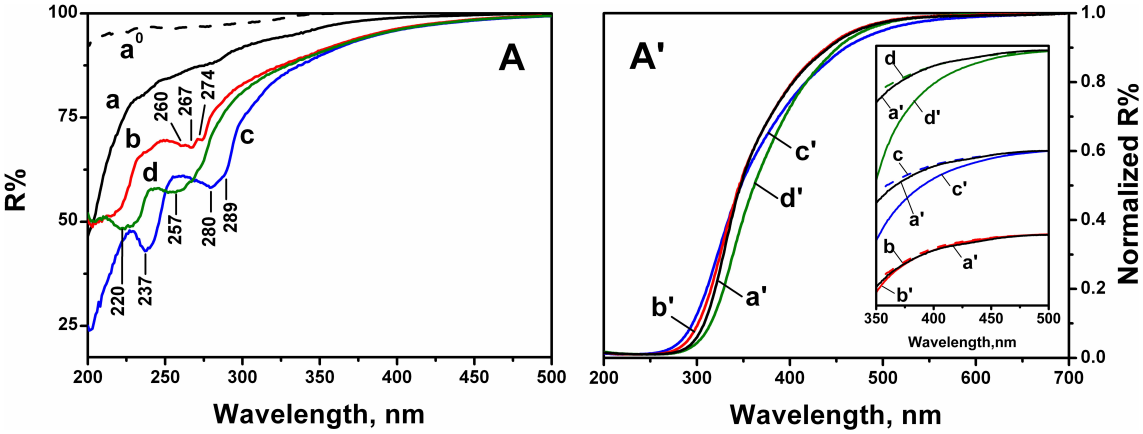
A
A'
R%
Normalized R%
Wavelength, nm
Wavelength, nm
Wavelength,nm
a0
a
b
c
d
220
237
257
260
267
274
280
289
a'
b'
c'
d'

Figure 3

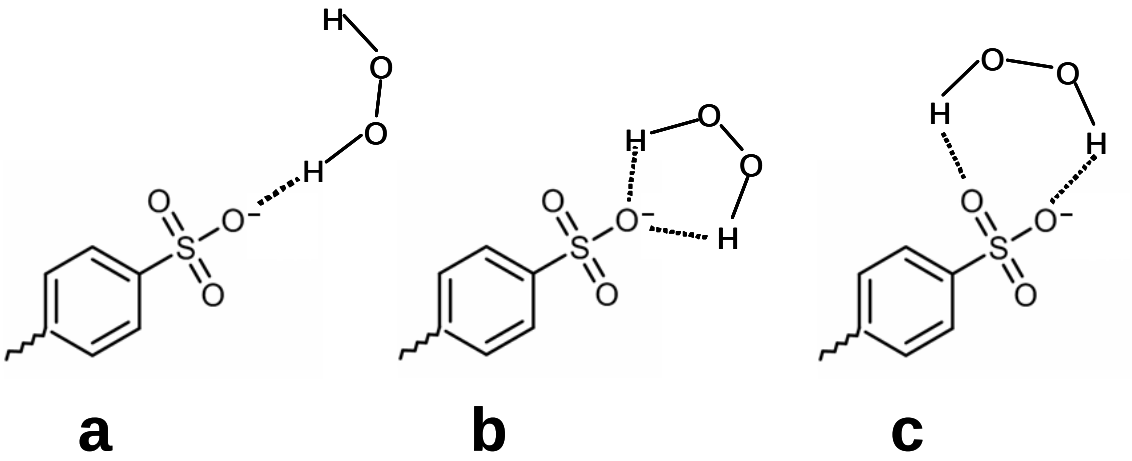

Figure 4

Table 1. Codes, textural features (SSA_{BET}, porosity) of the materials and catalytic efficiency of the supported sulfonic acids in the dihydroxylation of 1-methylcyclohexene.[a]

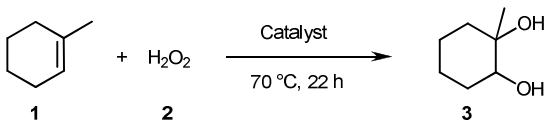

[a] Reaction conditions: 1-methylcyclohexene (0.5 mL, 4.2 mmol), 30% aq H_2O_2 (0.86 mL, 8.4 mmol), 70 °C, 22 h

Entry	Material	Specific surface area (m^2/g)	Total pore volume[b] (cm^3/g)	Average pore width[b] (nm)	Surf. acidity (mmol H^+/g)	Yield [Sel.][c] (%)
1	SiO_2	450	0.88	5.8	-	-
2	SiO_2-(C_6H_4)-SO_3H	440	0.87	5.8	0.65	80 [94]
3	SiO_2-$(CH_2)_3$-O-(C_6H_4)-SO_3H	415	0.80	5.3	0.70	55 [93]
4	SiO_2-$(CH_2)_2$-(C_6H_4)-SO_3H	300	0.43	4.2	1.20	90 [96]
5	Amberlyst-15	53	-	-	4.70	55 [93]

[b] Measured on the desorption branch
[c] Determined by GC analysis

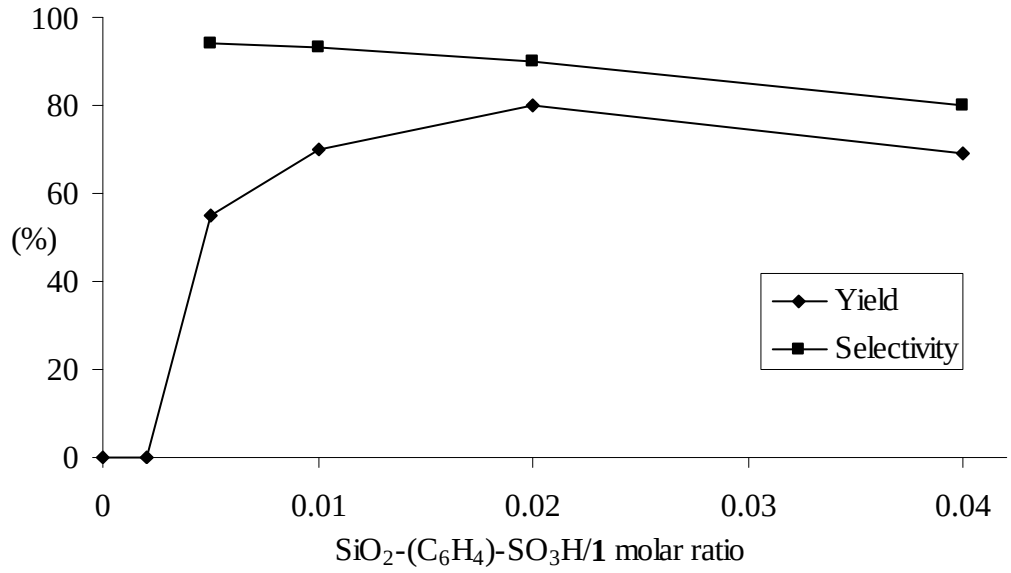
100
80
60
(%)
40
20
0
0
0.01
0.02
0.03
0.04
Yield
Selectivity
SiO2-(C6H4)-SO3H/1 molar ratio

Figure 5

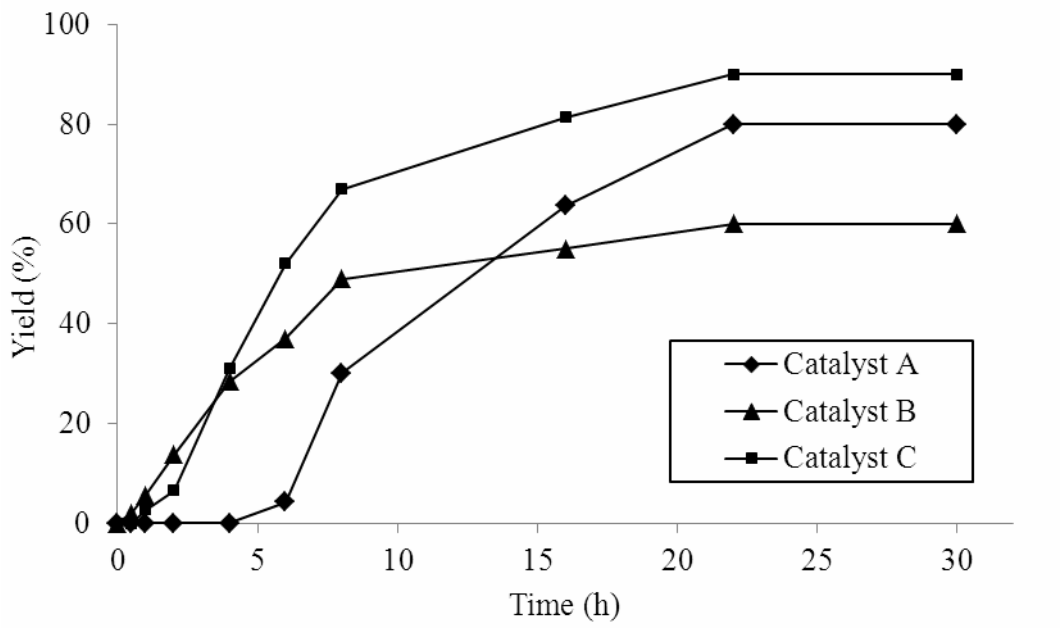
100
80
60
40
20
0
Yield (%)
0
5
10
15
20
25
30
Time (h)
Catalyst A
Catalyst B
Catalyst C

Figure 6

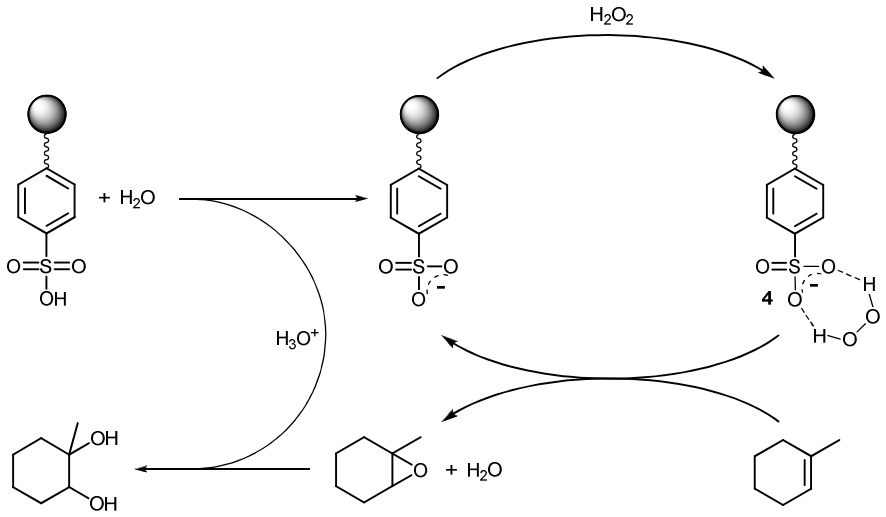

Scheme 1

Oxidation of alkenes to 1,2-diols: FT-IR and UV studies of silica-supported sulfonic acid catalysts and their interaction with H_2O and H_2O_2

Raimondo Maggi, Gianmario Martra, Calogero Giancarlo Piscopo,

Giovanni Sartori, Gabriele Alberto, Salvatore Coluccia

Supporting Information

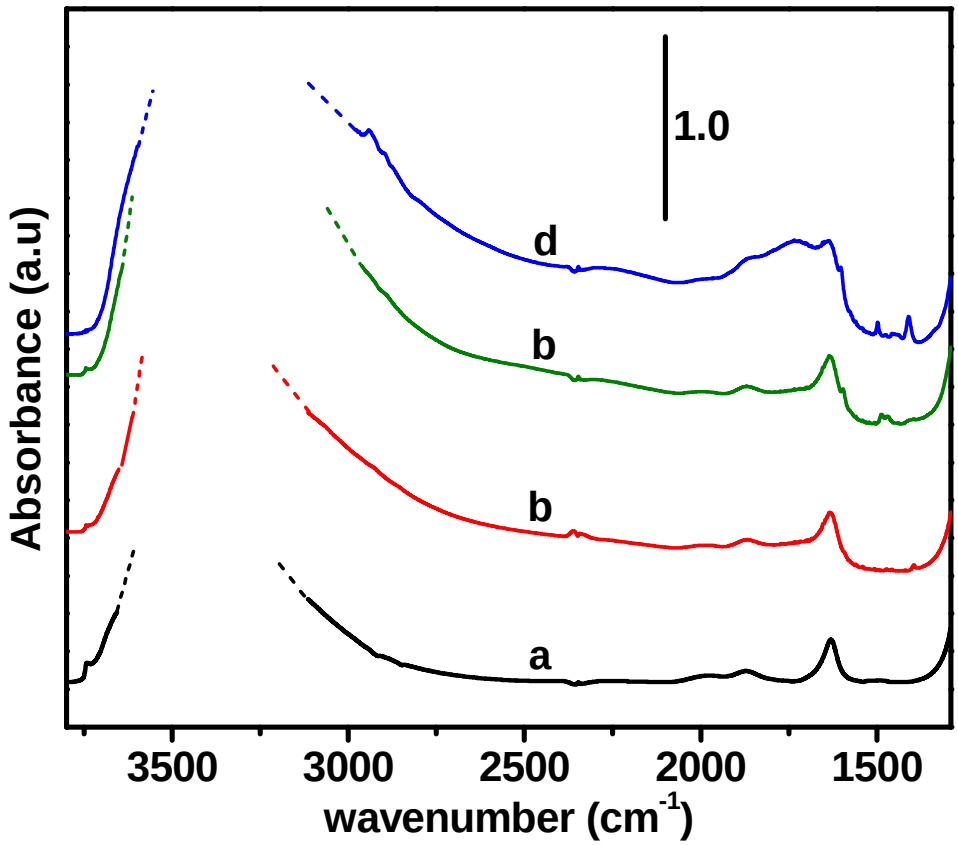

Figure SI-1. IR spectra of the samples in contact with air: a bare SiO_2; b) catalyst A; c) catalyst B; d) catalyst C. The maximum of the main absorption in the high frequency region was out of scale

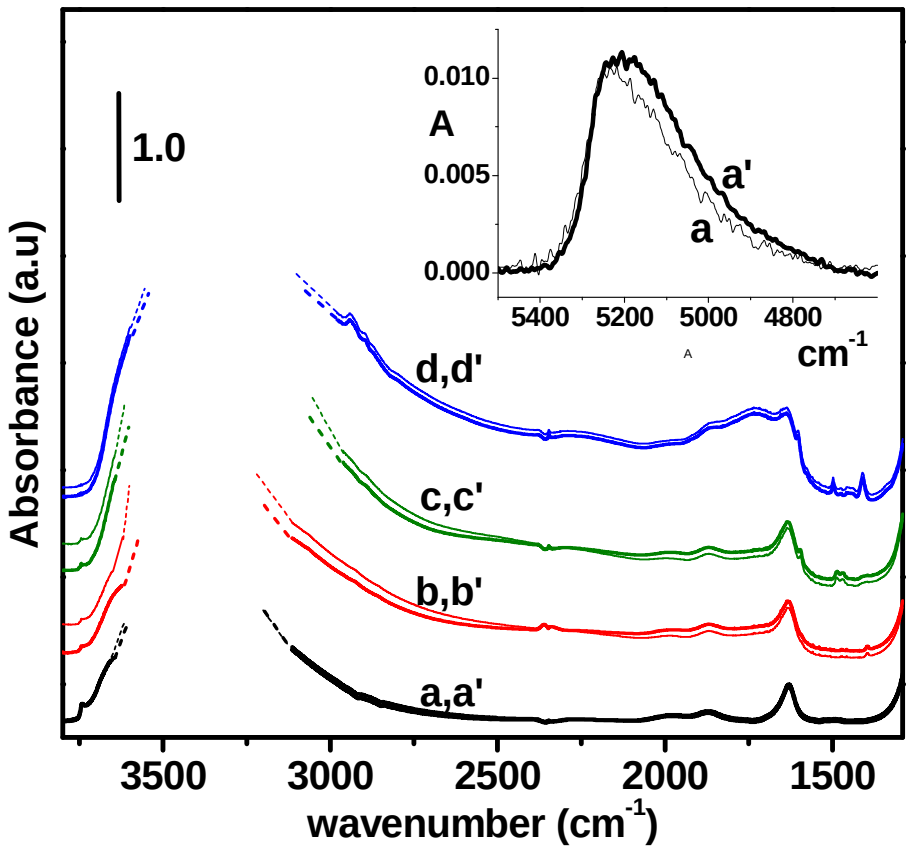

Figure SI-2. IR spectra of the samples in contact with 20 mbar of H_2O vapour (curves x) or of H_2O_2/H_2O (30% vol H_2O_2) (curves x'): a, a') bare SiO_2; b,b') catalyst A; c,c') catalyst B; d,d') catalyst C. The maximum of the main absorption in the high frequency region was out of scale. Inset: spectra, in the NIR region, of the bare SiO_2 in contact with 20 mbar of: a) H_2O; a') H_2O_2/H_2O (30% vol H_2O_2), as in the main frame. Similar data were obtained for the other samples.

Comment to Figure SI-2. No significant changes were observed between the spectra collected after admission on the samples of H_2O or H_2O_2/H_2O vapour. However, the presence of H_2O_2 in the liquid-like molecular layers formed on the sample surface was witnessed by the broadening towards the low frequency side of the $\nu_{OH}+\delta_{OH}$ band of water at 5230 cm^{-1} (NIR region), likely due to the presence of an additional component due to the same combination mode of H_2O_2 [1] (see inset).

[1] L.G.Weyer, S.-C. Lo, Handbook of Vibrational Spectroscopy, J.M. Chalmers, P.R. Griffiths (Eds), Wiley, Chichester 2003, Volume 3, p. 1832

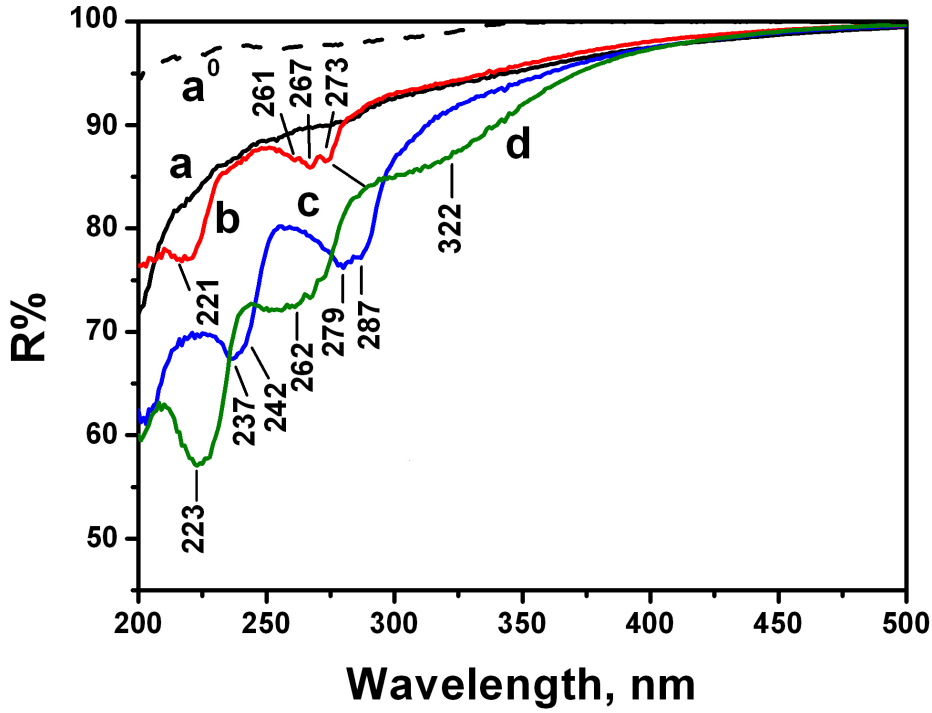

Figure SI-3. DR UV-Vis of samples in air: a^0) pyrogenic silica used as diluents; a) bare silica support; b) catalyst A; c) catalyst B; d) catalyst C.